

Original Article

He-Wei Granule enhances anti-tumor activity of cyclophosphamide by changing tumor microenvironment

Jianxiu Zhai, Zehai Song, Hang Chang, Yuwei Wang, Na Han, Zhihui Liu, Jun Yin *

Key Laboratory of Northeast Plant Materials, Department of Pharmacognosy and Utilization, School of Traditional Chinese Medicine, Shenyang Pharmaceutical University, Shenyang 110016, China

ARTICLE INFO

Article history:

Received 13 September 2020

Revised 15 November 2020

Accepted 12 March 2021

Available online 7 October 2021

Keywords:

cyclophosphamide

He-Wei Granule

H22 carcinoma

synergistic effect

toxicity

ABSTRACT

Objective: He-Wei Granule (HWKL) is a modern product derived from the modified formulation of traditional Chinese medicine Banxia Xiexin Decoction (BXD), which remarkably enhanced the anti-proliferation activity of cyclophosphamide (CTX) on HepG2 and SGC-7901 cell lines *in vitro* in our previous research. The aim of the study was to investigate the synergistic effects of HWKL and CTX using a transplanted H22 hepatocellular carcinoma mouse model.

Methods: The CTX-toxic-reducing efficacy of HWKL was evaluated by hematology indexes, organ indexes and marrow DNA detection. To investigate the underlying mechanisms, histopathology test, immunohistochemistry test and TUNEL staining were conducted. The efficacy of HWKL on the micro-vessel density (MVD) in tumor tissue was also evaluated by measuring CD34 level.

Results: High dose HWKL (6.75 g/kg) markedly attenuated CTX-induced hepatotoxicity and myelosuppression while significantly enhanced CTX anticancer efficacy *in vivo*. Further mechanism investigation suggested that high dose HWKL significantly increased cleaved Caspase 3 level and promoted apoptosis in tumor tissue by up-regulating Bax expression and down-regulating Bcl-2 and FasL expressions. Compared with CTX alone group, the decrease in LC-3B and Beclin 1 levels suggested that the autophagy in H22 carcinoma was significantly inhibited with addition of high dose HWKL. ELISA assay results indicated that the autophagy inhibition was achieved by decreasing p53 expression, blocking PI3K/AKT/mTOR pathway and recovering Th1/Th2 cytokine balance. In addition, CD34 and EGFR immunohistochemistry assay suggest that high dose HWKL could significantly decrease micro-vessel density (MVD) and inhibit angiogenesis in H22 carcinoma.

Conclusion: It can be concluded that high-dose HWKL enhanced CTX efficacy by promoting apoptosis, inhibiting autophagy and angiogenesis in tumor tissue while significantly alleviated CTX-induced toxicity, and could be applied along with CTX in clinical treatment as a supplement agent.

© 2021 Tianjin Press of Chinese Herbal Medicines. Published by ELSEVIER B.V. This is an open access article under the CC BY-NC-ND license (<http://creativecommons.org/licenses/by-nc-nd/4.0/>).

1. Introduction

As a major global public health problem, cancer is the leading cause of death among the world, with chemotherapy as its major therapeutic option. Alkylating anticancer drug cyclophosphamide (CTX) is an effective and commonly applied anticancer drug (Binotto, Trentin, & Semenzato, 2003; Emadi, Jones, & Brodsky, 2009). Unfortunately, patients receiving CTX have also been suffering from its serious side effects, such as myelosuppression and hepatic toxicity, while benefiting from its anticancer efficacy (De Jonge, Huitema, Rodenhuis, & Beijnen, 2005; Emadi et al., 2009). With the results provided by recent pre-clinical and clinical stud-

ies, traditional Chinese medicine (TCM) has been found with excellent supportive effects when combined with conventional chemotherapeutic drugs. It was found that the combination usage of TCM could increase the efficacy of chemotherapeutics while reduce the side effects, therefore improve patients' life quality and survival span (Qi et al., 2015; Su et al., 2014). Therefore, some Chinese herbal medicines such as PHY906, Huachansu Injection, and Kanglaite Injection are commonly applied among cancer patients currently (Lam et al., 2015).

He-Wei Granule (HWKL) is a modern product derived from the modified formulation of TCM Banxia Xiexin Decoction (BXD), it consists of seven herbs namely: *Pinellia ternate* (Thunb.) Breit., *Zingiber officinale* Rosc., *Panax ginseng* C. A. Mey., *Scutellaria baicalensis* Georgi., *Coptis chinensis* Franch., *Glycyrrhiza uralensis* Fisch. and *Ziziphus jujuba* Mill. In our previous studies, HWKL was observed

* Corresponding author.

E-mail address: yinjun826@sina.com (J. Yin).

with significant protective effects against cisplatin-induced nausea, vomiting, nephrotoxicity and myelosuppression (Song, Chang, Han, Liu, Liu, et al., 2017; Song, Chang, Han, Liu, Wang, et al., 2017). A total of 37 major components were identified using UHPLC-Q-TOF-MS/MS, among which ginsenosides, alkaloids, flavonoids, gingerols and polysaccharides were recognized as the principal compounds (Song et al., 2017). In our preliminary experiments, it was found that HWKL showed marked synergistic effects by enhancing the anti-proliferation activity of CTX on HepG2 and SGC-7901 cell lines when applied *in vitro*. In order to evaluate the synergistic effects of HWKL and CTX *in vivo* and to investigate the underlying mechanism, a transplanted H22 hepatocellular carcinoma model was established in mouse in this study.

2. Materials and methods

2.1. Materials

Fetal bovine serum and RPMI-1640 medium were purchased from Dalian Meilun Biology Technology Co., Ltd (Dalian, China). CTX was purchased from Shanxi Powerdone Pharmaceuticals Co., Ltd (Shanxi, China). Antibodies of Bax, Bcl-2, cleaved Caspase 3, Fas, FasL, TNF- α , IL-2, Beclin 1, p53, LC3B and CD34 were purchased from Wuhan Servicebio Technology Co., Ltd (Wuhan, China). Elisa kits for murine IL-2, IL-4, IL-6, IL-13, IFN- γ , TNF- α , cleaved Caspase 3, cleaved caspase 8, cleaved Caspase 9, EGFR, Beclin 1, AMPK, PTEN, PI3K, AKT and m-TOR and BCA total protein kit were purchased from Shanghai Yuan-Mu Biomedical Company (Shanghai, China). Kits for determining ALT, AST, GSH-Px, SOD and MDA were purchased from Nanjing Jiancheng Bioengineering Institute (Nanjing, China). All other reagents were of highest purity and commercially available by Shenyang Lab Science and Trade Co., Ltd (Shenyang, China). H22 tumor cell line (H8D8) was obtained from associate Prof. Ming-yu Xia of Department of Pharmacological in Shenyang Pharmaceutical University (Shenyang, China).

2.2. Preparation of HWKL and BXD

All the crude herbal drugs were purchased from Shenyang Guo-Da Pharmacy (Shenyang, China) and were confirmed as genuine medicinal materials by Prof. Jun Yin of Department of Pharmacognosy in Shenyang Pharmaceutical University. Preparation of HWKL and BXD was accomplished by Beijing Handian Pharmaceutical Institute (Beijing, China) by using the standard procedure in Fig. S1.

2.3. Animals treatment

A total of 88 KM (Kunming) mice (half male and half female) weighing 18–22 g were purchased from Liaoning Changsheng Biotechnology Company (Benxi, China) and group-housed under controlled temperature [(22 \pm 2) °C] and photoperiods (12 h: 12 h light–dark cycle). After 7 d acclimatization period, eight mice (half male and half female) were randomly selected as the control group. Other 80 mice were inoculated with 1×10^7 viable H8D8 cells subcutaneously on the left armpit. Twenty-four hours after inoculation, 80 mice were randomly divided into the following 10 groups ($n = 8$) namely: model group, CTX group (50.0 mg/kg, i.v.), BXD group (2.7 g/kg, i.g.), HWKL-D group (1.7 g/kg, i.g.), HWKL-Z group (3.4 g/kg, i.g.), HWKL-G group (6.8 g/kg, i.g.), CTX + HWKL-D group (50 mg/kg CTX i.v. + 1.7 g/kg HWKL i.g.), CTX + HWKL-Z group (50 mg/kg CTX i.v. + 3.4 g/kg, i.g.) and CTX + HWKL-G group (50 mg/kg CTX i.v. + 6.8 g/kg HWKL i.g.). Details of drug administration methods were shown in Fig. S1B. All animals were free to access food and water during the whole experiment, and the body weight of experimental animals were

recorded every day. The doses of HWKL in this study were designed according to 0.5-fold (HWKL-D, 1.7 g/kg, i.g.), 1-fold (HWKL-Z, 3.4 g/kg, i.g.) and 2-fold (HWKL-G, 6.8 g/kg, i.g.) of the clinical application dosage, respectively, and the dosage of BXD (2.7 g/kg, i.g.) and CTX (50 mg/kg, i.v.) were equal to their clinical application, respectively (Chen et al., 2015; Emadi et al., 2009; Xue et al., 2011). All of the experimental protocols were approved by the Animal Care and Use Committee of Shenyang Pharmaceutical University (SYPU-IACUC-C2016-0627–105).

2.4. Sample collection and preparation

At the last day of experiment (the 10th day), experimental mice were anesthetized with 4% chloral hydrate (10 mL/kg), blood was drawn from the *retro*-orbital vein and centrifuged at 4000 rpm for 15 min at 4 °C, the supernatant was kept for further hematology analysis.

After blood collection, the mice were then euthanized. Tissue samples, including hepatic lobule, spleen, thymus, marrow and femurs (right side) were then collected for further analysis. The collected tumors, spleens and thymuses were firstly washed with 4 °C saline then weighted. A partial of tumors were then fixed in 10% formalin for at least 24 h and were then embedded in paraffin. Other tumor tissues along with all the hepatic lobules were immersed in 9-fold volume of 0.9% saline and grounded into powder in ice-bath by Scientz-III ultrasonic cell disruption system (Ningbo Scientz Biotechnology Co., Ltd, Ningbo, China). The homogenates were centrifuged at 6000 rpm for 8 min at 4 °C to remove insoluble material, and the supernatant was kept for further analysis.

2.5. Evaluation of synergistic effect among drugs

The synergistic effect between drugs was calculated using the inhibitory rate of each drug according to formula 1. The inhibition rate was calculated according to tumor tissue weight.

$$(f_a)_{1,2} = 1 - [1 - (f_a)_1] \times [1 - (f_a)_2] \quad (1)$$

$(f_a)_1$ and $(f_a)_2$ are the inhibitory rate of drug 1 and drug 2, respectively. $(f_a)_{1,2}$ is the theoretical inhibitory rate of drug 1 with drug 2. $(f_b)_{1,2}$ is the actual inhibitory rate of drug 1 with drug 2. Synergistic effect is considered to be existed if $(f_b)_{1,2}$ is larger than $(f_a)_{1,2}$.

2.6. Hematology assay

The collected blood samples were used for hematology analysis by determining the levels of white blood cell (WBC), red blood cell (RBC), hematocrit (HCT) and hemoglobin (HGB) using a Nihon Kohden MZK-6318 blood analyzer (Japan).

2.7. Organ indexes and marrow DNA detection

Organ indexes: Spleens and thymuses were weighted to calculate organ index. The calculating formula was as follows.

$$\text{Organ index} = \text{organ weight (mg)} / (\text{body weight} - \text{tumor weight}) / (\text{per } 10 \text{ g}) \quad (2)$$

Marrow DNA detection: An intact right femur was washed with 10 mL 0.005 mol/L CaCl₂ solution. The solution was kept at 4 °C for 30 min and then centrifuged at 2500 rpm for 15 min. The supernatant was discarded and the residue was mixed with 5 mL 0.2 mol/L HClO₄ solution, vortexed for 1 min and then placed in

boiling water bath for 15 min. The solution was cooled and filtered. The filtrate was measured at 260 nm by ultraviolet spectrophotometer (UV-1200, AOE instrument, Shanghai, China).

2.8. Oxidative stress assessment

To assess the oxidative level in liver and tumor tissues in mice, the contents of MDA and activities of GSH-Px and SOD were determined using biochemical analysis kits according to the manufacturer's instructions. The absorbance of each sample was measured at 532 nm (MDA), 412 nm (GSH-Px) and 550 nm (SOD) respectively with a microplate reader (Thermo Scientific L-117, USA). Standard curves were prepared using diluted standard solutions to allow calculation of the relative target in the samples. All standards and samples were run in duplicate.

2.9. ELISA analysis

The supernatant fractions of tumor and hepatic lobule were analyzed with ELISA kits to determine the contents of IL-2, IL-4, IL-6, IL-13, IFN- γ , TNF- α , cleaved Caspase 3, cleaved Caspase 8, cleaved Caspase 9, EGFR, AMPK, PTEN, PI3K, AKT and m-TOR and BCA. The absorbance of each sample was measured at 450 nm with a microplate reader (Thermo Scientific L-117, USA). Standard curves were prepared using diluted standard solutions to allow calculation of the relative target in the samples. All standards and samples were run in duplicate.

2.10. Histopathology staining

After fixation, paraffin-fixed tumor tissues were sectioned (5 μ m thickness), and slides were stained with haematoxylin and eosin. Representative microphotographs were obtained with a light microscope (Nikon, Japan).

2.11. Immunohistochemistry and TUNEL assay

After fixation, paraffin-fixed tumor tissues were sectioned (5 μ m thickness), and the 5 μ m thick deparaffinized tissue sections were rehydrated with a series of xylene and aqueous alcohol solutions. The deparaffinized tumor slices were incubated overnight at 4 °C with primary antibodies against Bax, Bcl-2, cleaved caspase 3, Fas, FasL, TNF- α , IL-2, Beclin 1, p53, LC3B and CD34. The slices were then incubated with biotin-labeled secondary antibodies and streptavidin-HRP for 50 min at room temperature. Immunoreactivity was detected using 3–3'-diaminobenzidine (DAB), followed by counterstaining with hematoxylin. Localization of positive staining was analyzed by light microscopy.

Cellular apoptosis in tumor tissue was assessed using a terminal deoxynucleotidyl transferase dUTP nick end-labeling assay kit (TUNEL, Roche, Sigma-Aldrich). In brief, following dewaxing and hydration, tumor sections were digested with proteinase K for 30 min and labeled with a TUNEL reaction mixture for 2 h at 37 °C. TUNEL apoptosis index was measured by the following method. Five positive views of each sample were selected by assessing positive cells in each section ($\times 400$). The apoptosis index of each view was calculated as the average ratio of view/total cells attained from four views.

2.12. MVD scoring

The CD34-stained sections were observed and photographed under a light microscope equipped with a digital camera (Olympus BX51TF, Tokyo, Japan). The images of the sections were processed by cellSens Standard 1.4.1 software (Olympus, Japan) according to a counting procedure reported by Foote et al (Foote et al., 2005).

Briefly, micro-vessel density (MVD) was determined in views which contained the highest numbers of microvessels per area. In each view, a single countable microvessel was considered to be observed as a group of endothelial cells (or an endothelial cell cluster) which were positive for CD34 (brown staining) and were clearly separated from an adjacent cluster. Five views were obtained from each sample, and the value of MVD was calculated as the mean of five views.

2.13. Statistical analysis

Statistical analysis was performed using the statistical software SPSS 19.0. Data were expressed as mean \pm SD. Comparisons between two groups were performed using one-way ANOVA followed by LSD test in the condition of variance homogeneity or Dunnett T3 test in the case of variance heterogeneity. Differences between groups were considered statistically significance at $P < 0.05$.

3. Results

3.1. HWKL administration enhances antitumor activity of CTX against H22 tumor

According to the histological staining results, tumor tissue from model group were observed with significant features of malignancy, such as huge nucleus, malalignment, high ratio of nucleus to cytoplasm, deeper stained nucleus, unclear demarcation between parenchyma and mesenchyme, and large amount of tumor giant cells. Compared with model group, obvious cell death and cell vacuolation were found in the tumor tissue from other groups (Fig. 1A), and it was found that the administration of CTX, CTX + HWKL-D, CTX + HWKL-Z and CTX + HWKL-G reduced tumor weight by 72.7%, 80.3%, 80.5% and 88.2%, respectively (Fig. 1B, $P < 0.05$). Compared with CTX alone group, the tumor inhibition rate in HWKL-G + CTX group was significantly increased by 61.1%. According to formula (1), synergistic effect was observed in CTX + HWKL-G group, which indicated that an enhanced antitumor efficacy could be achieved with the combination of CTX and high dose HWKL (Table 1).

3.2. HWKL administration reduced CTX-induced toxicity in mice

Also, it was found that HWKL administration significantly attenuated CTX-induced toxicity. The bodyweight of mice from CTX along group decreased significantly compared with control group, and the decrease was reversed by HWKL administration in a dose-dependent manner (Fig. 1D). After CTX treatment, thymus index and absorbance of marrow DNA were significantly decreased which suggested CTX might induce myelosuppression (Fig. 2A and B). The results of spleen index and hematological indexes (WBC, RBC, HCT and HGB) also support the conclusion (Fig. 2 and Fig. 3). What's more, CTX treatment caused an increase in ALT and AST content by 0.4- and 7.6-fold compared with model group, which indicated liver damage (Fig. 3A). The decrease of GSH-Px and SOD activities (Fig. S2) along with the increase in MDA content (Fig. 4B) in serum and liver suggested that CTX-induced myelosuppression and hepatotoxicity might be related to oxidative damage. With high dose HWKL administration, the activity of GSH-Px and SOD were significantly recovered in CTX-treated mice, while MDA content was decreased by 20.7% (Fig. 4 B–D, $P < 0.05$). The results suggested that HWKL could significantly reduce the CTX-induced myelosuppression and hepatotoxicity through down-regulating oxidative stress level.

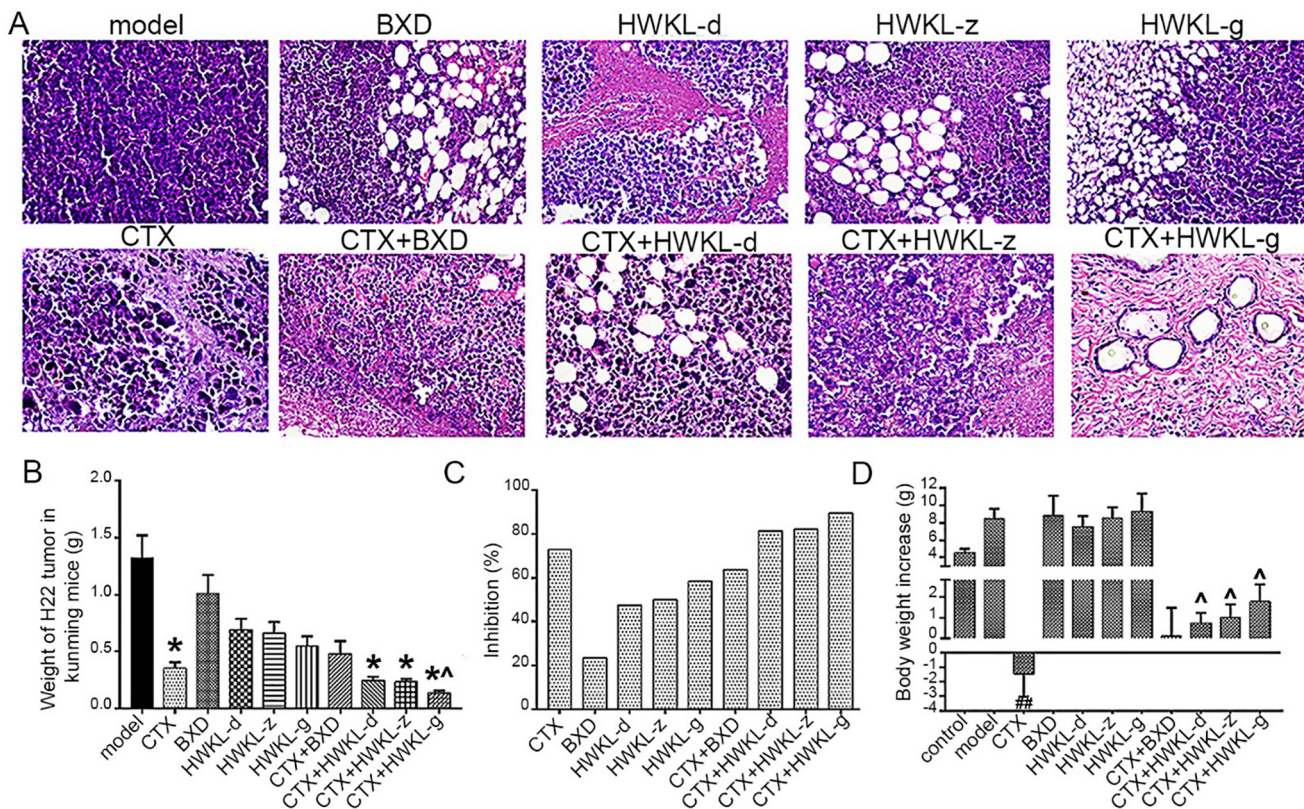


Fig. 1. Pathological features of transplanted tumors in mice bearing H22 hepatocellular carcinoma after different treatments (×400, A). Weight of H22 tumor in different groups (B, mean ± SD, n = 8). Inhibition effects of each drug on H22 hepatocellular carcinoma in the mice (C). Bodyweight increase of the mice in different groups (D) (mean ± SD, n = 8). *P < 0.05 vs model group. ^P < 0.05 vs CTX alone group.

Table 1
Synergistic effect of drugs.

Groups	Doses (g/kg)	Animals		Tumor weight/g	(f _a) _{1,2}	(f _b) _{1,2}	Synergistic effects
		Day 0	Day 11				
Control		8	8				
Model		8	7	1.32 ± 0.22			
CTX	0.05	8	7	0.36 ± 0.056		73.06	
BXT	2.07	8	7	1.01 ± 0.18		23.45	
HWKL-D	1.6875	8	8	0.69 ± 0.098		47.48	
HWKL-Z	3.375	8	8	0.66 ± 0.10		50.11	
HWKL-G	6.75	8	8	0.55 ± 0.092		58.45	
CTX + BXXXT	0.05 + 2.07	8	7	0.48 ± 0.012	79.38	63.71	No
CTX + HWKL-D	0.05 + 1.6875	8	8	0.24 ± 0.045	85.85	81.48	No
CTX + HWKL-Z	0.05 + 3.375	8	8	0.23 ± 0.029	86.56	82.33	No
CTX + HWKL-G	0.05 + 6.75	8	8	0.14 ± 0.021	88.81	89.53	Yes

(f_b)_{1,2} was the actual inhibitory rate of drug 1with drug 2.
Synergistic effect was considered to be existed if (f_b)_{1,2} was larger than (f_a)_{1,2}.

3.3. HWKL administration increased apoptosis in CTX-treated H22 tumors

When compared with CTX alone group, the combination of HWKL and CTX significantly promoted apoptosis in H22 tumors, which was indicated by an increase in TUNEL apoptosis index and cleaved Caspase 3 content. Compared with the model group, the tunnel apoptosis indexes of CTX group, HWKL-G group and three combination drug therapy groups were significantly increased by 77.7%, 63.6%, 81.8%, 113.6%, and 122.7% (Fig. 5A). Compared with CTX alone group, the apoptosis index of HWKL-

G + CTX group significantly increased by 25.6% (P < 0.05). It was also found that with the combination of high dose HWKL and CTX administration, the expression of Bax, FasL were significantly increased compared with CTX alone group by 19.3% and 25.0%, while the expression of Bcl-2 was down-regulated by 21.4% (Fig. 5 B–D, P < 0.05). The increase in cleaved Caspase 8 and cleaved Caspase 9 contents, two upstream proteins of Caspase 3, indicated that both death receptor and mitochondria-mediated apoptosis were involved in the process (Fig. 6). The immunochemistry results of all indexes attained from each group were shown in Figs. S3–S6.

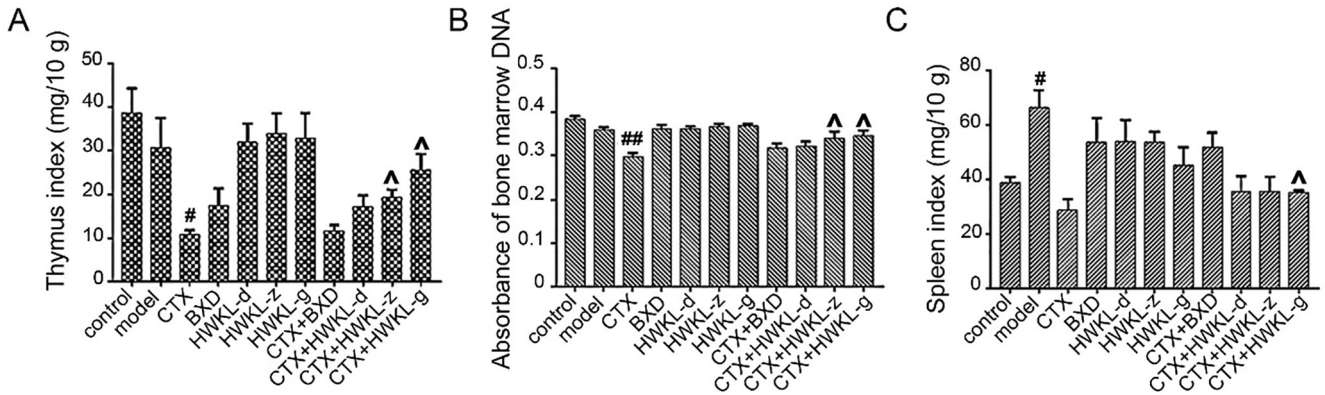


Fig. 2. Effects of CTX, BXD and HWKL administration on: thymus index (A), absorbance of marrow DNA (B), spleen index (C) of experiment mice, * $P < 0.05$, ** $P < 0.01$ vs control group. ^ $P < 0.05$ vs CTX alone group (mean \pm SD, $n = 8$).

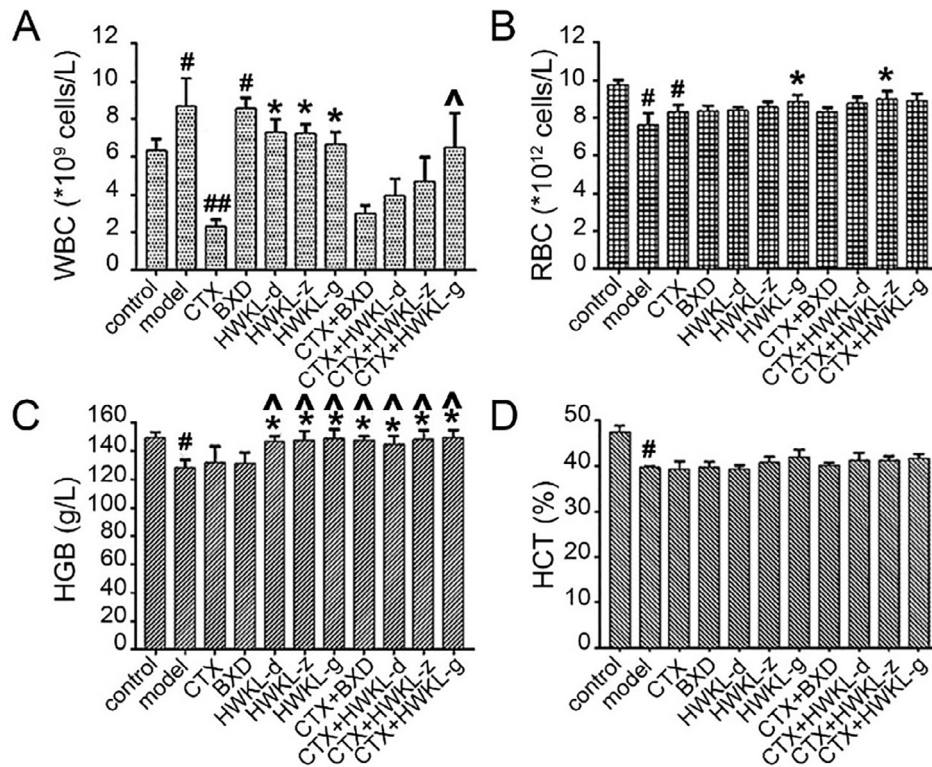


Fig. 3. Effects of CTX, BXD and HWKL administration on the hematological indexes of (A) white blood cell (WBC), (B) red blood cell (RBC), (C) hemoglobin (HGB) and (D) hematocrit (HCT) of experiment mice. * $P < 0.05$, ** $P < 0.01$ vs control group. ^ $P < 0.05$ vs model group. ^ $P < 0.05$ vs CTX alone group (mean \pm SD, $n = 8$).

3.4. HWKL administration inhibited autophagy in CTX-treated H22 tumors by regulating mutant p53 related indexes

Increased punctiform positive staining of LC-3B and Beclin 1 was found by immunohistochemistry in model group, which indicated autophagy. When compared with model group, the expressions of LC-3B, Beclin 1 and p53 in HWKL-G + CTX group were significantly reduced ($P < 0.01$). When compared with CTX alone group, HWKL-G + CTX treatment significantly down-regulated the expressions of LC-3B, Beclin 1 and p53 by 37.1%, 38.6% and 28.6%, respectively (Fig. 7A, $P < 0.01$). Meanwhile, with p53 overexpression, the PTEN and AMPK levels were up-regulated in tumor tissues from model group, which could promote autophagy

(Fig. 7B). In addition, the expression levels of PI3K, AKT and mTOR were found to be significantly up-regulated by CTX + HWKL-G treatment when compared with model group as well as CTX alone group (Fig. 7B). The immunochemistry results of all attained from each group were shown in Figs. S7–9.

3.5. HWKL administration improved ratio of Th1/Th2 cytokines in H22 tumors

Compared with CTX alone group, the combination of HWKL administration increased the content of Th1 cytokines, such as IFN- γ , TNF- α and IL-2. Among all doses, high dose HWKL showed the most potent effect, and up-regulated TNF- α and IL-2 levels

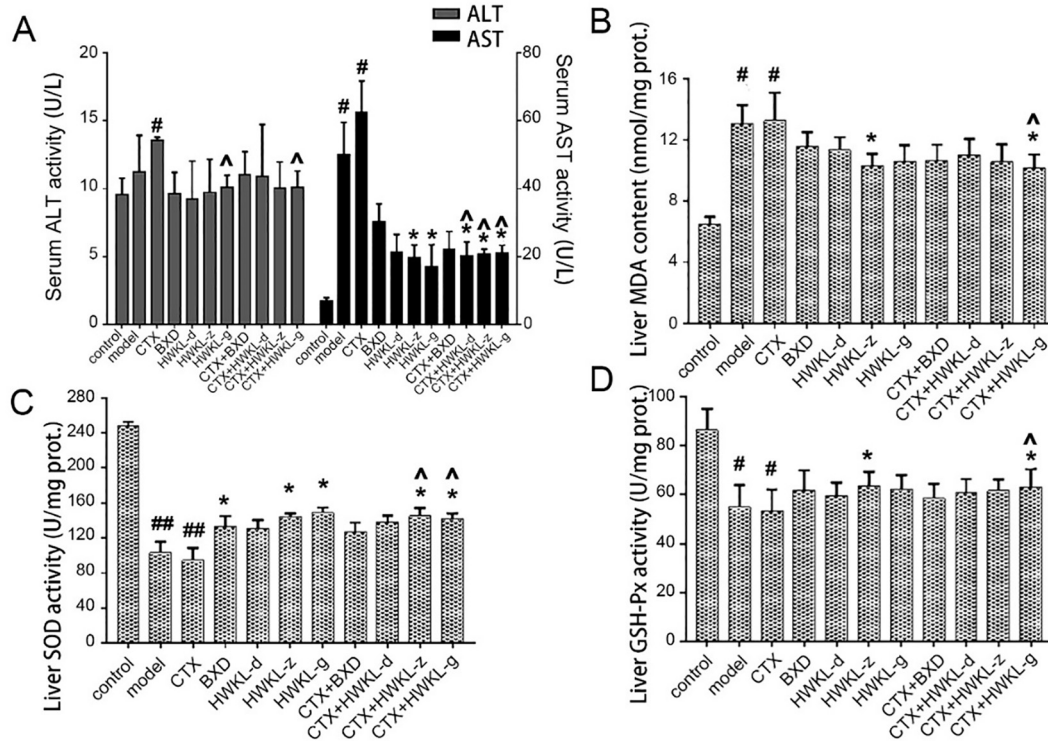


Fig. 4. Effects of CTX, BXD and HWKL administration on: ALT and AST activities (A), hepatic MDA content (B), hepatic SOD activity (C), and hepatic GSH-Px activity (D). #*P* < 0.05, ##*P* < 0.01 vs control group. **P* < 0.05 vs model group. ^*P* < 0.05 vs CTX alone group (mean ± SD, *n* = 8).

by 25.6% and 16.7% (*P* < 0.05). However, compared with model group and CTX alone group, the contents of Th2 cytokines, such as IL-4, IL-6 and IL-13 were respectively reduced by 16.9%, 30.2% and 23.6% when CTX was administrated along with high dose HWKL (Fig. 8, *P* < 0.05).

3.6. HWKL reduced angiogenesis in H22 tumors

Angiogenesis was observed in the model group as indicated by an increase in CD34 and micro-vessel density (MVD). Compared with model group and CTX alone group, the expression of CD34 was significantly reduced by 31.4%, 34.3% and 42.9% in combination treatment group (HWKL-D + CTX, HWKL-Z + CTX, HWKL-G + CTX, *P* < 0.05) (Fig. 9). Also, HWKL + CTX administration significantly reduced MVD in H22 tumor tissue, with high dose HWKL showing the most potent effect (reduced by 31.3%, *P* < 0.05), indicating that HWKL could enhance the antitumor activity of CTX by inhibiting angiogenesis. In comparison with the model group and the CTX group, the content of EGFR in the CTX + HWKL-Z group and CTX + HWKL-G group was markedly reduced.

4. Discussion

It was found that single-dose HWKL exhibited moderate activity on inhibiting tumor growth. However, combined HWKL administration significantly enhanced the inhibitory effects of CTX against H22 tumor by promoting apoptosis, inhibiting autophagy, regulating T cell cytokines and inhibiting angiogenesis. Meanwhile, HWKL effectively attenuated CTX-induced hepatotoxicity and myelosuppression. This study first systemically studied the effects and possible mechanisms of HWKL on anticancer aspect, and the attained results indicated that HWKL had the value as a supplementary drug in cancer treatment.

In our previous study, HWKL was found to significantly attenuate cisplatin-induced nausea, vomiting, nephrotoxicity and myelosuppression in rats (Song, Chang, Han, Liu, Liu, et al., 2017; Song, Chang, Han, Liu, Wang, et al., 2017). Results attained from this study indicate that the combination of HWKL administration could also attenuate CTX-induced toxicity. Compared with CTX alone group, the combination of HWKL-D, HWKL-Z and HWKL-G significantly reversed body weight loss (Fig. 1D). Hematology assay results suggested that the CTX-induced myelosuppression was significantly attenuated in HWKL-G + CTX group (Fig. 2 and Fig. 3). Also, the addition of high dose HWKL was found to significantly decrease CTX-induced hepatotoxicity by down-regulating oxidative stress in liver (Fig. 4).

As shown in Fig. 1B, single-dose HWKL administration showed little effect on inhibiting H22 tumor growth when compared with CTX alone group. However, the anti-tumor efficacy of CTX was remarkably enhanced when combined with HWKL administration. Results from TUNEL immunohistochemistry assay indicated that the combination of high dose HWKL could significantly promote apoptosis in tumor tissue (Fig. 5A). According to previous reports, CTX induces tumor cell apoptosis mainly through two pathways, namely mitochondria-dependent pathway and death receptor pathway (Lee, Park, & Yang, 1997; Simões-Wüst, Schürpf, Hall, Stahel, & Zangemeister-Wittke, 2002). In mitochondria-dependent pathway, the activation of the pro-apoptotic gene Bax leads to the release of apoptosis activator cytochrome-C from the mitochondria, thereby activating cell death (Ho et al., 2015; Lee et al., 1997). However, the anti-apoptotic protein Bcl-2 could combine with Bax, stabilizing mitochondrial membrane and block the release of cytochrome-C. Compared with CTX alone group, the combination of high-dose HWKL and CTX significantly up-regulated the expression of Bax while decreased Bcl-2 expression (Fig. 5B and C). In the death receptor pathway, the combination of Fas and FasL could lead to cell apoptosis (Camagna et al.,

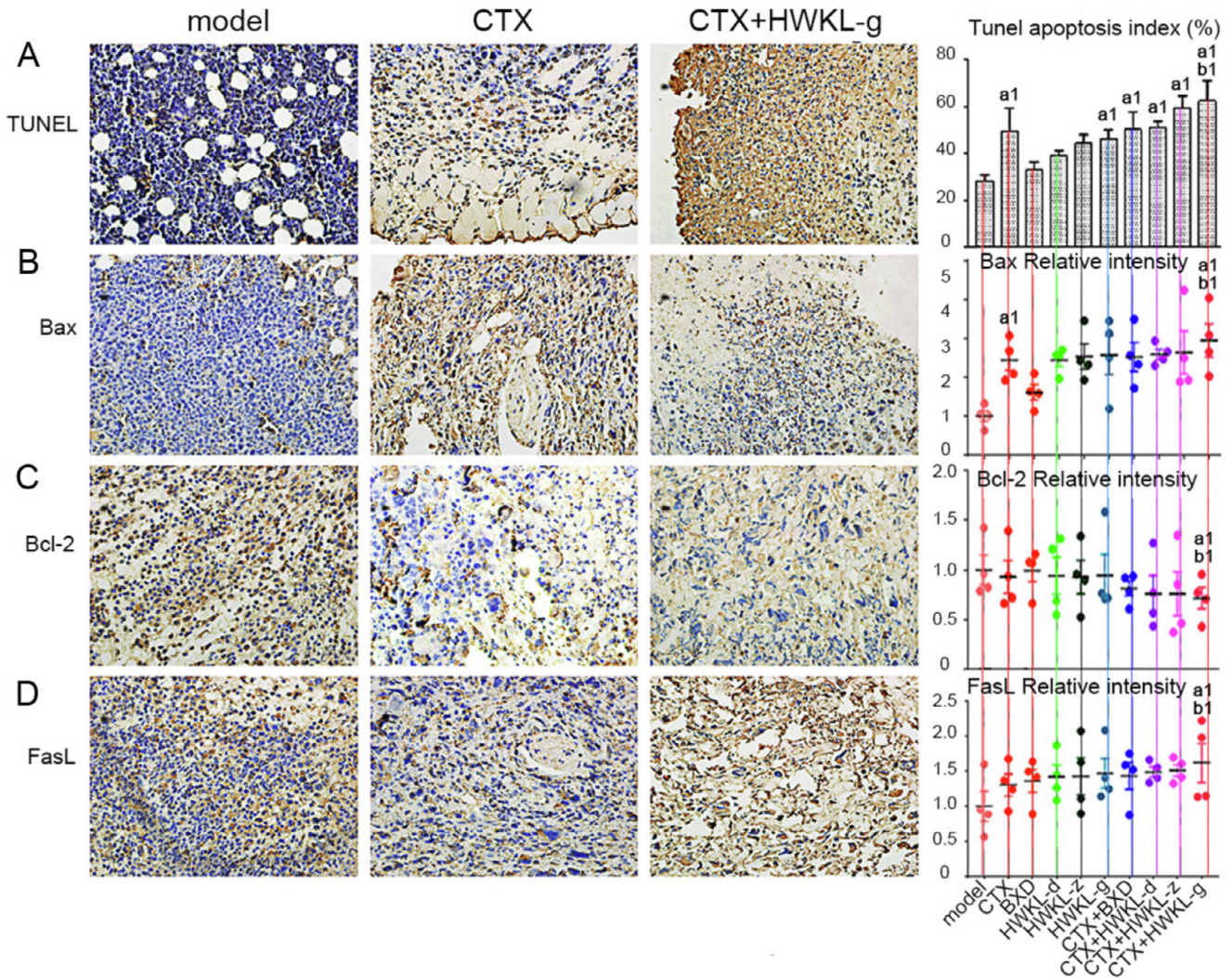


Fig. 5. Effects of HWKL and CTX treatment on cell apoptosis in mice H22 tumor using immunohistochemical assay. (A) TUNEL apoptosis assay, (B) Bax, (C) Bcl-2, (D) FasL. ^{a1}*P* < 0.05, vs model group. ^{b1}*P* < 0.05 vs CTX alone group (mean ± SD, *n* = 8).

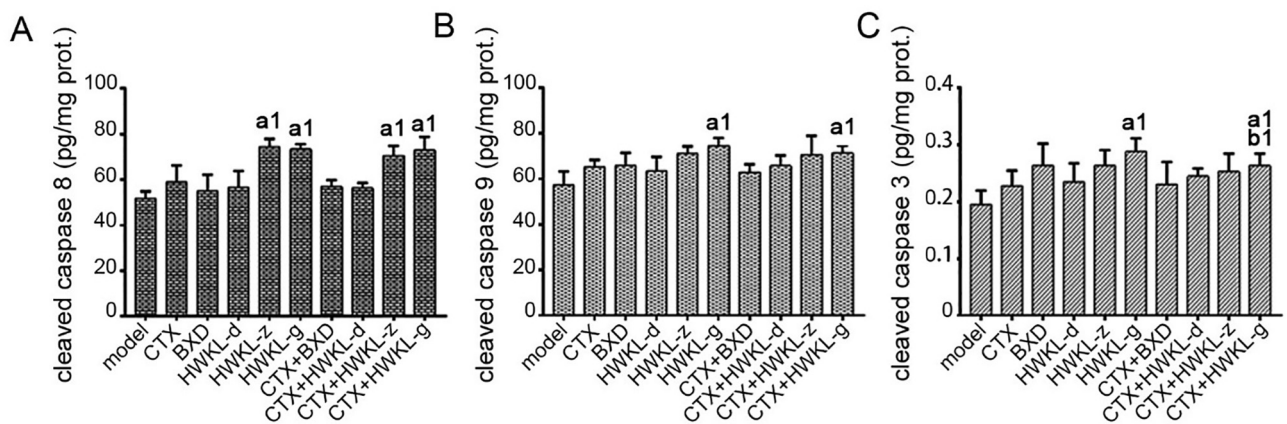


Fig. 6. Effects of HWKL, BXD and CTX treatment on contents of cleaved Caspase 8 (A), cleaved Caspase 9 (B) and cleaved Caspase 3 (C) in mice H22 tumor using ELISA assay. ^{a1}*P* < 0.05 vs model group. ^{b1}*P* < 0.05 vs CTX alone group (mean ± SD, *n* = 8).

2015). With the combination of high-dose HWKL, the expression of FasL was significantly increased (Fig. 5D) while Fas remained unaffected (data not shown). By affecting the above two pathways, the

combination of high dose HWKL and CTX remarkably increased the levels of cleaved Caspase 8 and cleaved Caspase 9 compared with model group (Fig. 6). As the downstream protease of Caspase 8

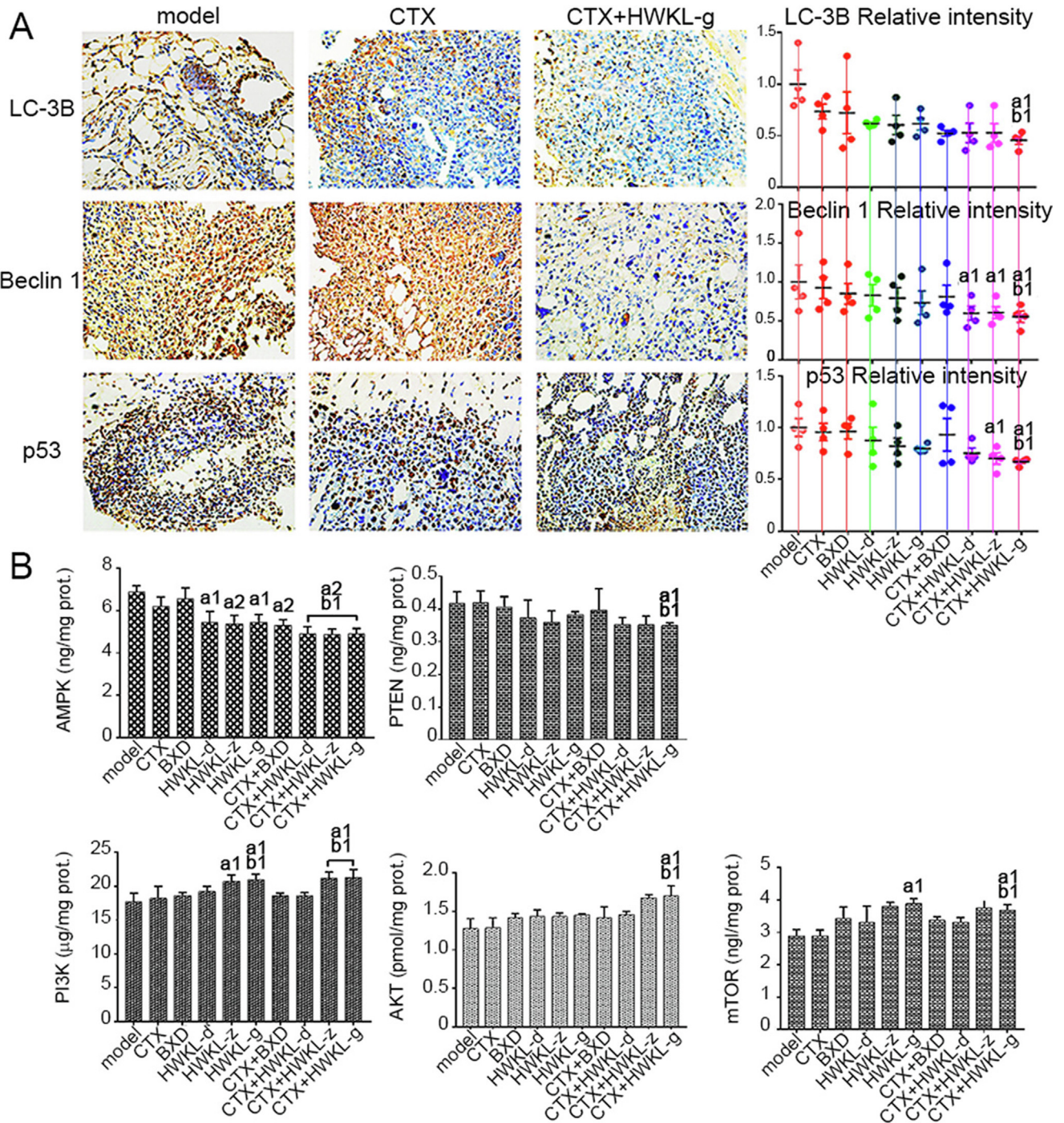


Fig. 7. Protein expression levels of autophagy related markers and mutant p53 in mice H2T tumors (A). Contents of AMPK, PTEN, PI3K, AKT and mTOR in mice H2T tumors (B). ^{a1}*P* < 0.05, ^{a2}*P* < 0.01 vs model group. ^{b1}*P* < 0.05 vs CTX alone group (mean ± SD, *n* = 8).

and 9 (Volate et al., 2010), Caspase 3 expression was markedly reduced by HWKL-G + CTX treatment. It was found that the level of cleaved Caspase 3 in HWKL-G + CTX group was significantly higher than model group and CTX alone group, indicating that high dose HWKL showed good synergistic effect with CTX treatment, which was supported by synergistic investigation (Table 1). From the results attained above, it could be speculated that HWKL showed good supporting efficacy in CTX treatment by affecting mitochondria-dependent and death receptor pathways.

Except for apoptosis, it was found that HWKL could also enhance CTX efficacy by inhibiting tumor cell autophagy, because the expression levels of autophagy-related gene Beclin 1 and LC-3B were significantly decreased by HWKL-G combined administration compared with CTX alone group (Fig. 7A) (Chen, Jiang, Huang, Liu, & Yu, 2013; Fu, Cheng, & Liu, 2013). What's more, it was found that HWKL-G combined administration could also significantly increase the expression level of metastasis inhibitor mTOR compared with CTX alone group (Fig. 7B) (Jiang et al., 2015), suggesting

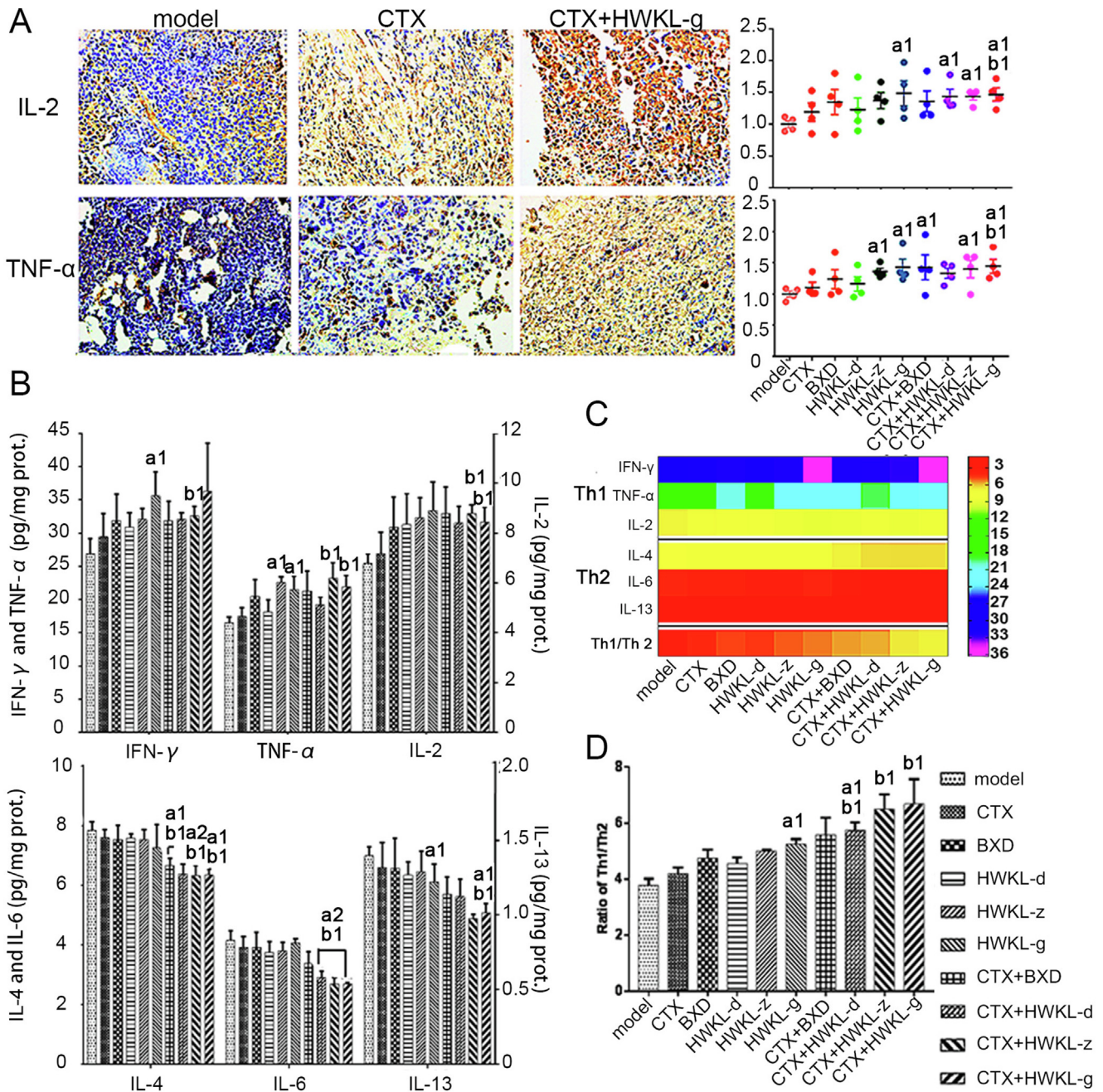


Fig. 8. Effect of HWKL administration on ratio of Th1/Th2 cytokines in H22 tumors (mean \pm SD, $n = 8$). The protein expression levels of IL-2 and TNF- α in mice H22 tumors (A), The contents of IFN- γ , TNF- α , IL-2, IL-4, IL-6 and IL-13 in mice H22 tumors (column diagram) (B), The ratio of Th1/Th2 cytokines (heat map) (C), The ratio of Th1/Th2 cytokines (column diagram) (D). ^{a1} $P < 0.05$, ^{a2} $P < 0.01$ vs model group. ^{b1} $P < 0.05$ vs CTX alone group.

that HWKL-G might inhibit metastasis in H22 transplanted mice. Compared with model group and CTX alone group, mice received HWKL-G administration exhibited remarked lower expression of p53, AMPK and PTEN as well as significantly higher PI3K, AKT and mTOR expressions (Fig. 7). The above results indicated that HWKL administration might regulate mTOR expression by activating PI3K/AKT/mTOR signaling pathway (Jr & Janku, 2014; Liu, Mao, Garnett, Bogler, & Yung, 2008). In addition, the disruption of Th1/Th2 cytokine balance has been also recognized as the sigh of metastasis (Wada et al., 2007). Compared with model group, it has been observed that HWKL-G + CTX treatment markedly recovered Th1/Th2 level by decreasing Th1 cytokine levels (namely IFN-

γ , TNF- α , and IL-2) and increasing Th2 cytokine levels (namely IL-4, IL-6 and IL-13) (Fig. 8). Meanwhile, HWKL-G treatment also inhibited angiogenesis in tumor tissue compared with CTX alone treatment. Using immunohistochemistry assay, the combination of high dose HWKL and CTX was found to significantly decreased CD34 expression in tumor tissue, decreasing MVD level and the expression of EGFR (Fig. 9).

Although preliminary conclusions were attained in this study, there are still limitations that need to be further investigated. The major effective components of HWKL remain to be determined. Moreover, it was unknown that if HWKL possesses synergistic effect with other anti-cancer agents.

- Song, Z., Chang, H., Han, N., Liu, Z., Wang, Z., Gao, H., & Yin, J. (2017). He-Wei granules inhibit chemotherapy-induced vomiting (CINV) in rats by reducing oxidative stress and regulating 5-HT, substance P, ghrelin and obestatin. *RSC Advances*, 7(69), 43866–43878.
- Su, X., Dong, C., Zhang, J., Su, L., Wang, X., Cui, H., & Chen, Z. (2014). Combination therapy of anti-cancer bioactive peptide with Cisplatin decreases chemotherapy dosing and toxicity to improve the quality of life in xenograft nude mice bearing human gastric cancer. *Cell and Bioscience*, 4(1), 7.
- Volate, S. R., Kawasaki, B. T., Hurt, E. M., Milner, J. A., Kim, Y. S., White, J., & Farrar, W. L. (2010). Gossypol induces apoptosis by activating p53 in prostate cancer cells and prostate tumor-initiating cells. *Molecular Cancer Therapeutics*, 9(2), 461–470.
- Wada, H., Seki, S., Takahashi, T., Kawarabayashi, N., Higuchi, H., Habu, Y., Sugahara, S., & Kazama, T. (2007). Combined spinal and general anesthesia attenuates liver metastasis by preserving TH1/TH2 cytokine balance. *Anesthesiology*, 106(3), 499–506.
- Xue, R., Cao, Y., Han, N., Lin, X., Liu, Z., & Yin, J. (2011). Activity of DBXX granules on anti-gastric ulcer and decreasing the side effect of chemotherapy in S180 tumor-bearing mice. *Journal of Ethnopharmacology*, 137(3), 1156–1160.